Reinforced Concrete Wall under Shear Load – Experimental and Nonlinear simulation

Jiri Kala, Petr Hradil and Miroslav Bajer

***Abstract*—**Concrete-like materials models generally share in common some basic features of brittle materials such as pressure hardening, strain hardening and strain rate dependency. The elasto-plastic models are based on the condition of plasticity with the associative or non-associative plastic flow law. The modulus of elasticity of concrete is one of the most important parameters for determining the strain distributions and displacements. The numerical study was verified by an experiment carried out on the test specimen is a reinforced concrete wall with the dimensions 1000 mm x 1000 mm x 80 mm.

***Keywords*—**ANSYS, Non-linear brittle material, Shear skew, Reinforced Concrete wall, Test apparatus.

I. Introduction

CONCRETE is an important material in civil constructions. Concrete material has a complicated nonlinear behaviour that is difficult to be described for general stress conditions by a simple constitutive model. Due to advancement in the computing perform, it is now possible to apply numerical simulation for the response of concrete structures subjected to different time dependent load cases. Plenty of commercial systems such as AUTODYN, LSDYNA and ANSYS [2] with special material module MultiPlas [14] are available for the general simulation of structural nonlinear responses. However, in order for such simulations to produce reliable results regarding the response of a concrete structure, a sound material model capable of representing the essential mechanical processes of the material under varying stress and loading rate conditions is vital.

Concrete by nature is a heterogeneous material. Hence, modeling concrete at a meso-scale level, i.e., considering the heterogeneity of the material composition using, for example, the discrete element method (DEM) [19], is advantageous in depicting detailed mechanical processes of the material. However, the enormous computational demand associated with a meso-scale model could become prohibitive in solving practical problems [1,5]. Therefore, in general applications, concrete is often treated as homogeneous by the so-called macro-scale material models.

Numerous studies have been carried out in the last 20 years for the development and improvement of the macro-scale concrete models for high-pressure applications, e.g., [3,6,16,17]. Various material models have been proposed, from relatively simple to more sophisticated ones, and their capabilities in describing the actual nonlinear behaviour of the material under different loading conditions vary [9,13]. Besides, because of the general complexity of the models, the determination of the model parameters (i.e., the model parameterization) also plays an important role in the actual performance of these models. This requires a sufficient understanding of the modeling formulation and the associated considerations [7,12].

II. Review of Typical Concrete Material Models

A number of models for concrete-like materials have been developed. These models generally share in common some basic features of brittle materials such as pressure hardening, strain hardening and strain rate dependency [6]. However, for simplicity sake, some models adopt highly restrictive assumptions, consequently their applicability is limited to a certain class of problems. In cases where the loading environment of the material is very complex and cannot be pre-defined, more robust material models that are capable of describing the varying concrete material behaviours under different loading conditions are desired [4].

Distribution of material models for numerical simulations in FE software can be derived from the distribution of materials by their response to tensile stress. In this respect, the material models fall into three categories.

a) group of brittle response that includes glass.

b) group of elasto-plastic response, where plastics or steel and other metals can be incorporated.

c) group of quasi-brittle materials like plain concrete, reinforced concrete, prestressed concrete or fiber reinforced concrete and other materials with cementitious matrix.

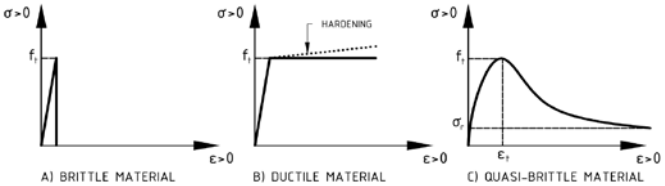

Fig. 1 Material by their response to the tensile stress

This result was achieved with the financial support of the project GACR 14-25320S "Aspects of the use of complex nonlinear material models"

Jiri Kala is with the Brno University of Technology, Faculty of Civil Engineering, Brno, 602 00 CZ (phone: +420-541147392; fax: +420-541147392; e-mail: kala.j@fce.vutbr.cz).

Petr Hradil is with the Brno University of Technology, Faculty of Civil Engineering, Brno, 602 00 CZ (e-mail: hradil.p@fce.vutbr.cz).

Miroslav Bajer is with the Brno University of Technology, Faculty of Civil Engineering, Brno, 602 00 CZ (e-mail: bajer.m@fce.vutbr.cz).

A. Concrete modelling using modified Drucker-Prager model

The elasto-plastic models are based on the condition of plasticity with the associative or non-associative plastic flow law. MultiPlas has an efficient and robust algorithm for material models with single-surface plasticity and multi-surface plasticity for use in the Finite Element Method analysis in ANSYS software. This is often employed in the case of models which include isotropic and anisotropic plasticity conditions.

The yield condition consists of two yield criteria (1), (2), [14] whereby the concrete strength can be described close to the reality in the compressive as well as in the tensile domain.

$$F_1 = \sigma_s + \beta_t \sigma_m - \tilde{\sigma}_{yt} \Omega_1 \quad (1)$$

$$\beta_t = \frac{\sqrt{3}(R_d - R_z)}{R_d + R_z},\ \tilde{\sigma}_{yt} = \frac{2R_d R_z}{\sqrt{3}(R_d + R_z)}$$

$$F_2 = \sigma_s + \beta_c \sigma_m - \tilde{\sigma}_{yc} \Omega_2 \quad (2)$$

$$\beta_c = \frac{\sqrt{3}(R_u - R_d)}{2R_u - R_d},\ \tilde{\sigma}_{yc} = \frac{R_u R_d}{\sqrt{3}(2R_u - R_d)}$$

where:

σ_m hydrostatic stress $\sigma_m = \frac{\sigma_x + \sigma_y + \sigma_z}{3}$

I_2 second invariant of the deviatoric main stresses

$\sigma_s = \sqrt{I_2}$

R_z uniaxial tensile strength

R_d uniaxial compression strength

R_u biaxial compression strength

Ω hardening and softening function (in the pressure domain $\Omega_1 = \Omega_2 = \Omega_c$, in the tensile domain $\Omega_1 = \Omega_t$).

The comparison with the concrete model made by [15] is shown in Fig. 2 and illustrates the advantages of the Drucker-Prager model consisting of two yield criteria. While there is a very good correspondence in the compressive domain, the chosen Drucker-Prager model can be well adjusted to the realistic tensile strength.

In contrast to that, the Ottosen model overestimates these areas significantly. A further advantage lies within the description of the yield condition using the three easily estimable and generally known parameters R_z, R_d and R_u.

In case of nonlinear deformation behaviour for the pressure load, the softening area is characterized by a decreasing strength, which leads to a low residual strain level. The slope of the decreasing branch is a measure for the brittleness of the material. Fig. 3 (top) shows the typical nonlinear stress-strain relation of normal concrete in uniaxial compressive tests (DIN 1045-1, 2001). In Fig. 3 (bottom), the stress-strain relation which is available in MultiPlas with modified Drucker-Prager model is shown. Thereby linear softening (m_{law} = 0, 2) or parabolic-exponential softening (m_{law} = 1) can be chosen. The parabola equation (as seen in Fig. 3 (top) is used until the strain ε_u is reached.

Under tensile load, concrete tends to soften relatively brittly with local appearances of cracks. In order to include this into the context of a continuum model, a homogenized crack and a softening model are needed. The crack itself does not appear in the topology description of the structure - but is described by its impact on stress and deformation state. The softening process is formulated respectively to the energy dissipation caused by the occurance of cracks.

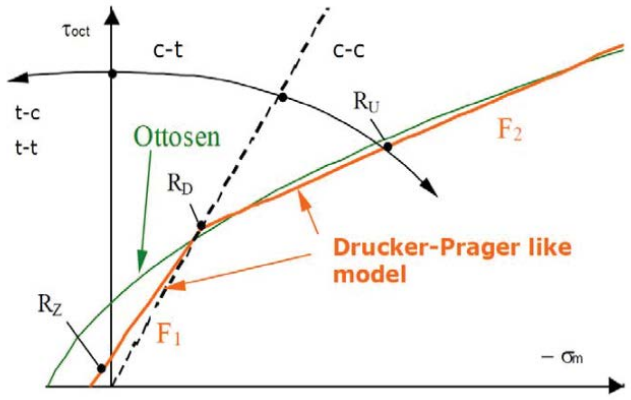

Fig. 2 – Modified Drucker-Prager condition of plasticity in an octahedral plane

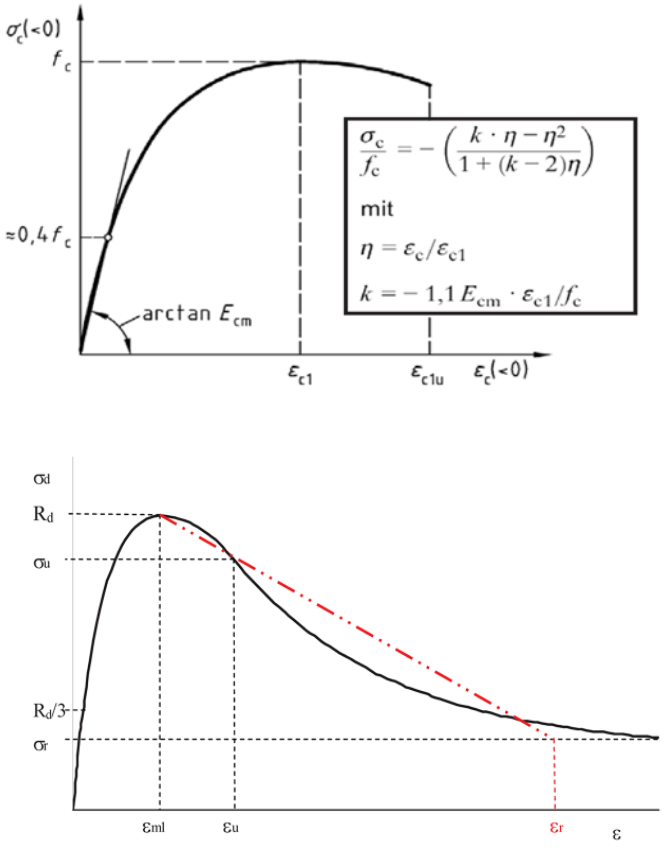

Fig. 3 – Nonlinear concrete model – diagram of concrete under pressure (top) and under tension (bottom) (MultiPlas, 2010; DIN 1045-1, 2001)

For the cracking to be complete, the fracture energy concerning the crack surface has to be dissipated. The model used is based on the crack band theory [3]. It states that cracks develop within a local process zone [10]. Its width hPR (crack band width) is a material specific constant. To avoid a mesh dependency of the softening and to assess the fracture energy correctly, a modification of the work equation is necessary [6].

III. Test Arrangement

The designed test apparatus is made up of a massive stiff steel frame, which simulates similar conditions to those existing when the test specimen is placed within a structure, see Fig. 4. The test specimen is a reinforced concrete wall with the dimensions 1000 mm x 1000 mm x 80 mm. The wall is reinforced by welded wire mesh across both surfaces. Within the test programme the shear capacity was stipulated for reinforced concrete elements damaged by flexural cracking, as well as those without cracks.

The wall is reinforced by a welded wire mesh across both surfaces. The welded wire mesh is made up of circle meshes with the thickness of 8 mm and mesh size of 100mm X 100mm. On both left and right vertical edges as well as on the upper horizontal edge, the wall element is fixed to the bearing steel plates. On the left edge, the horizontal wires of the welded wire mesh are lead through the holes in the steel bearing plate and welded on its outer surface, see Fig. 4. The remaining steel reinforcements always end on the edge of the reinforced concrete plate [8].

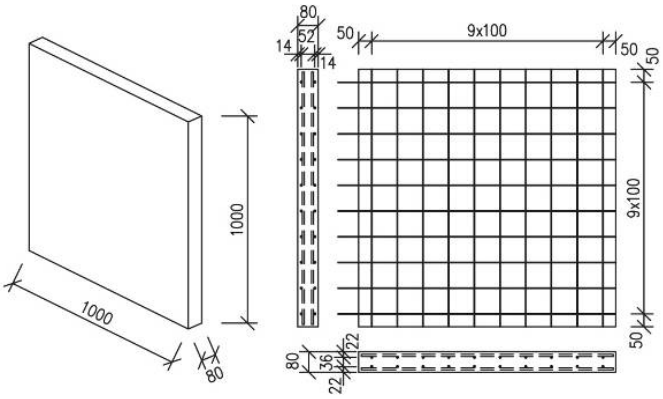

Fig.4 The reinforced wall element

Approximately a quarter of the area located in the bottom right corner of the wall element is fixed by a steel structure that acts against the deviation of the wall from its plane. This stabilization of the wall element is bolted to the lower steel profile of the steel frame. The mean values of the measured physical properties of concrete from ten specimens 100 x 100 x 400 mm (28 days) are:

density ρ= 2362 kg.m^{-3},
compressive strength f_c=43,8 MPa, and
modulus of elasticity E=28,817 GPa.

Fig. 5 – Photograph and schematic diagram of the test apparatus

The main part of the test apparatus is a closed steel frame, manufactured from HEB beams. The corners of the frame are connected by high-strength bolts. The steel frame lies on steel bearing plates and is vertically stabilized.

The vertical HEB beams are provided with steel foot plates on both sides. Thus, it is possible to create a bolt connection of vertical and horizontal steel beams using high-strength bolts. Each connection of a vertical and a horizontal HEB beam is created by eight M30 bolts of the strength of 10.9, with the exception of the part connecting also the arm. Here, eight M30 bolts of the stength of 10.9 are designed, as well.

The left side of the test specimen is connected to the frame in such a way that it enables the transmission of horizontal forces. This is ensured by gluing a steel plate to the surface of the concrete and by anchoring the overlapping reinforcement. The metal plate is attached to the frame along its height via

elements that transmit horizontal forces only. The total vertical force is transmitted from the lower part of the slab into the frame. The right side of the test specimen is placed so that it and the frame can slide mutually on each other. A Teflon layer that minimizes vertical friction is used in this area, placed in a steel plate connected to the frame by adjustable bolts.

Loading is created by a hydraulic loading device, which introduces loading to the upper part of the frame and via the load distribution arm to the test specimen. Loading took place in several loading and unloading cycles.

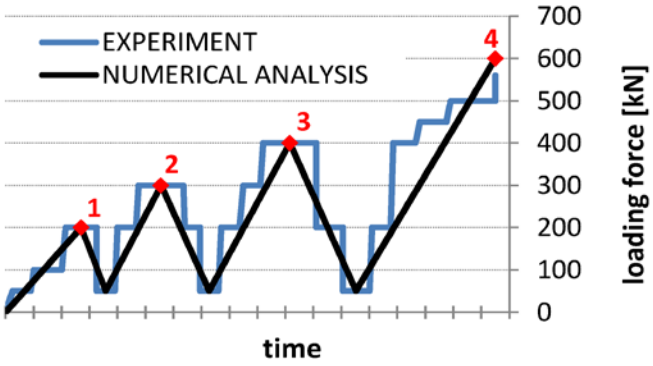

Fig.6 – Schematic diagram of cyclic loading

Two groups of data from the experiments were evaluated – data on the skewing of the wall element and on the force effects of elements on the test apparatus. Fig. 7 (top) shows the points at which the vertical displacements of the element were measured, the resulting values being used for the calculation of total skewing. These vertical displacements are measured as changes in the heights of the lower corners of the wall element, and thus the total skewing includes not only the skewing of the element itself, but also the rotation of the element caused by the deformation of the steel frame of the test apparatus. The skewing of monitored sections (0.2 m x 0.2 m) was also measured, these sections being defined on the surface of the wall element, see Fig. 7 (centre). These instances of skewing were assessed from the changes in the lengths of verticals, horizontals and diagonals in each monitored section, and thus express shear deformation without the influence of deformation of the frame. The effects of the wall element on the steel frame were measured using a a load gauge and are represented by the horizontal forces H1, H2,… , H8 and the vertical force R (the total force transferred from the test specimen to the frame), see Fig.7 (bottom).

IV. Computational Model

In order to simulate shear wall loading tests a spatial finite element model was created of the wall element and the test apparatus in ANSYS technology using concrete material model from MultiPlas module. This model correctly describes the nonlinear behaviour of the reinforced concrete element and the stiffness of the test apparatus, as well as their mutual interaction. A configuration was used for the calculations in which the wall element was not damaged by flexure cracking.

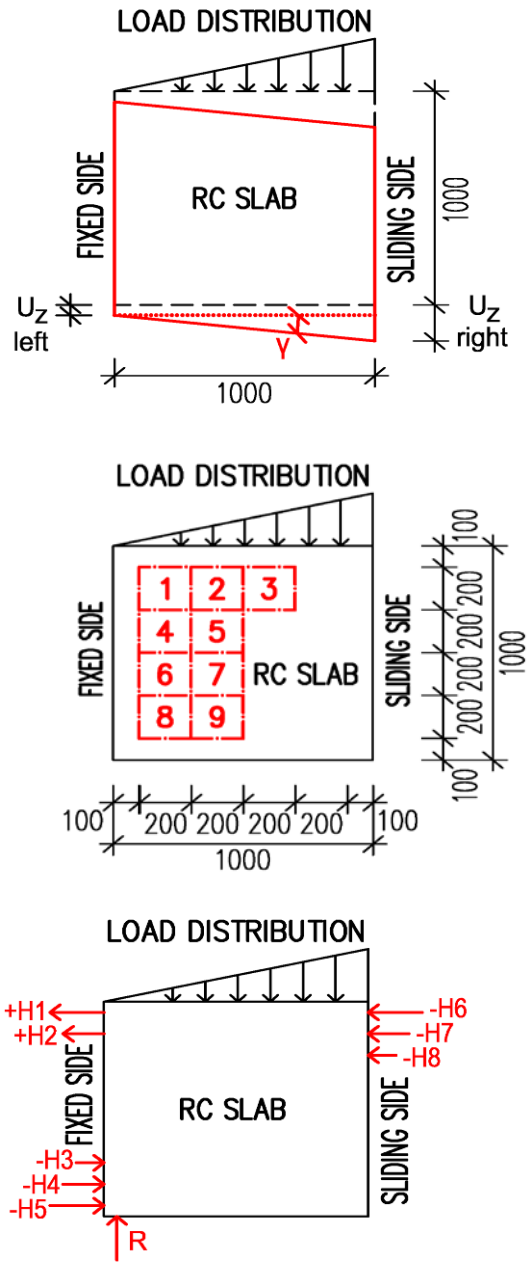

Fig. 7 – Shear deformation (skewing) of the wall element (top); a schematic diagram of the monitored sections on the surface of the wall element (centre); force effects exerted by the element on the frame (bottom)

The spatial geometry of the wall element is formed from elements of the SOLID45 type with a nonlinear material model of concrete, described in section 2. Element SOLID45 is used for the 3-D modeling of solid structures. The element is defined by eight nodes having three degrees of freedom at each node: translations in the nodal *x*, *y*, and *z* directions. The reinforcement of the reinforced concrete wall is made up of LINK8 idealised elements with a multilinear elasto-plastic material model of steel. The 3-D spar element is a uniaxial tension-compression element with three degrees of freedom at

each node: translations in the nodal *x*, *y*, and *z* directions. As in a pin-jointed structure, no bending of the element is considered.

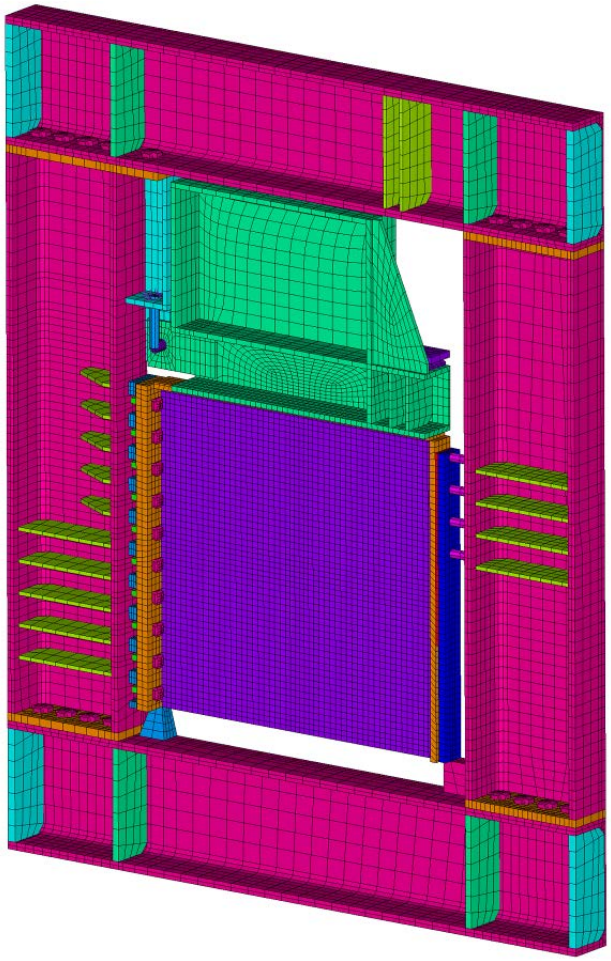

Fig.8 – Finite element model of the test apparatus

The steel frame composed of HEB beams is discretized by SOLSH190 spatial elements. Element SOLSH190 is used for simulating shell structures with a wide range of thickness (from thin to moderately thick). The element possesses the continuum solid element topology and features eight-node connectivity with three degrees of freedom at each node: translations in the nodal x, y, and z directions. Thus, connecting SOLSH190 with other continuum elements requires no extra efforts.

The high-strength bolts in the corners of the frame are modelled using LINK8 elements with presstressing. On the interfacial surfaces of the HEB beams there are contact elements modelled in such a way that they transmit only pressure. The frame lies on steel bearing plates, with contact defined at their interface [11].

On the left side (firmly fixed) a steel load distribution plate is attached to the tested element. The connection of this plate to the steel frame is modelled by LINK8 rod elements, which transmit horizontal forces only. Vertical force from the distribution plate is transmitted through the stiff coupling into the lower part of the steel frame. The slide assembly on the right side is modelled by SOLSH190 elements, which make up the steel plate and the Teflon strip layer. A nonlinear frictionless interface is defined between the steel plate and the Teflon strip. The material model of the Teflon strip is described by an elasto-plastic diagram. The connection of the slide assembly to the frame is modelled by rod elements which transmit only pressure.

The arm for the distribution of loading is discretized by SOLSH190 elements. The hinged arm assembly is modelled by BEAM4 rod elements and linear binding equations. Element BEAM4 is a uniaxial element with tension, compression, torsion, and bending capabilities. The element has six degrees of freedom at each node: translations in the nodal *x*, *y*, and *z* directions and rotations about the nodal *x*, *y*, and *z* axes.

V. Conclusions, Discussion

The results obtained from the numerical simulation demonstrate a very good correlation with the data measured during the experiment.

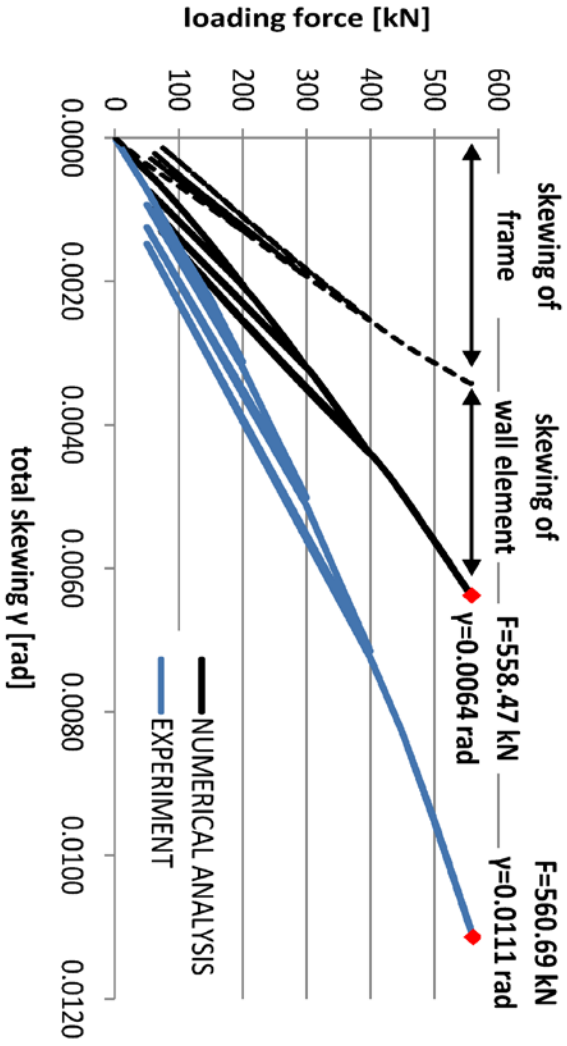

Fig. 9 – Dependence of the total skewing of the wall element on the loading force

The maximal calculated force transmitted through the specimen (558 kN) is close to the measured value (561 kN). The calculated progression of the total skewing of the element dependent on the loading force is compared with the measured results in Fig.9.

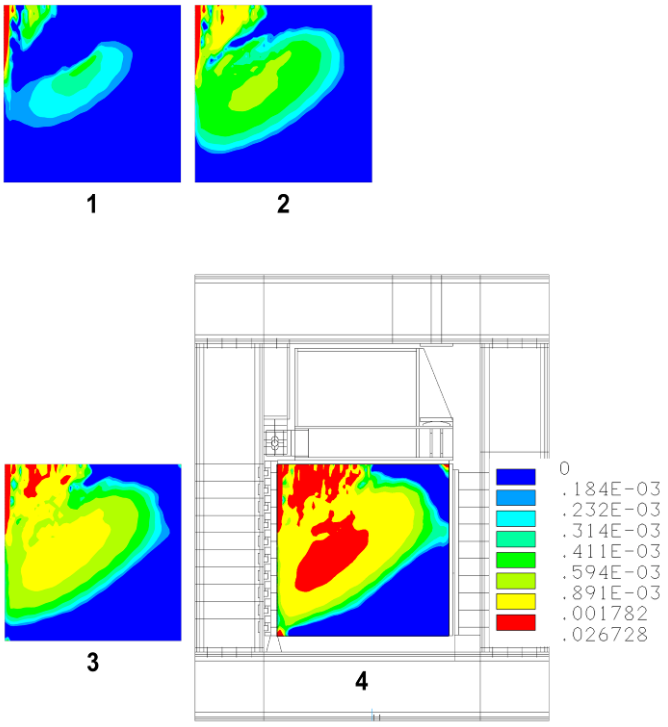

Fig.10 – Maximal main plastic deformation of the wall element

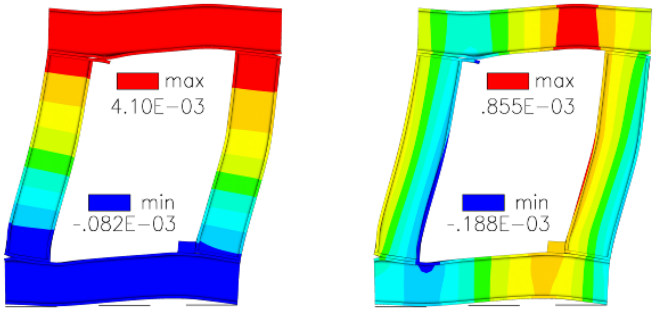

Fig.11 – Horizontal displacement of the steel frame (left), vertical displacement (right), [enlarged 100x]

The used spatial computational model provides detailed information on the behaviour of the tested specimen and test apparatus. Fig. 10 shows the maximal main plastic deformation of a wall element in individual loading steps. The displacement of the frame in the horizontal and vertical directions is depicted in Fig. 11.

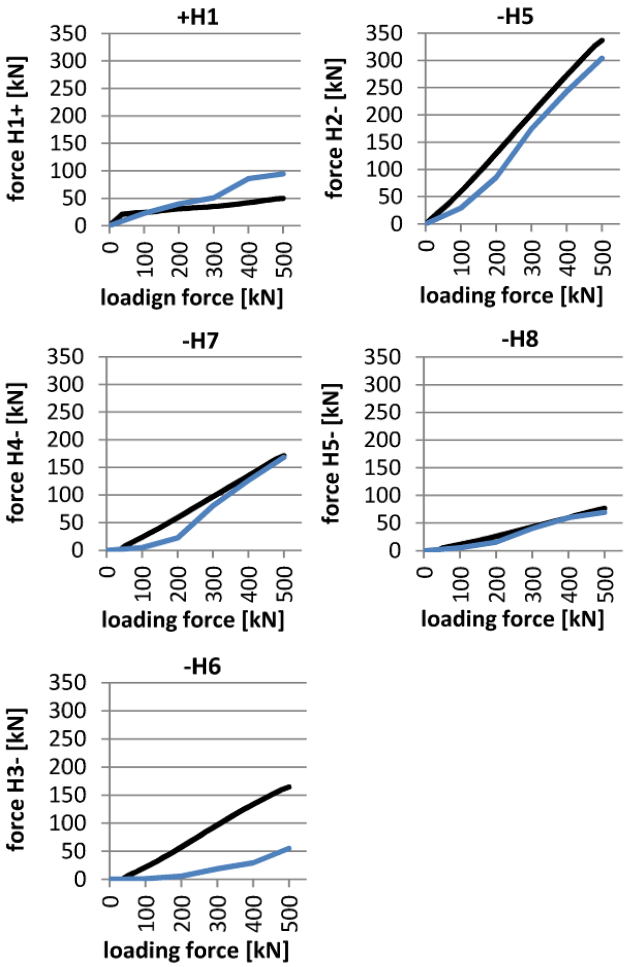

Fig.12 – Records of edge horizontal forces showing dependence on loading

The calculated skewing is lower than the experiment showed. This may be due to the differences in the calculated and measured horizontal forces between the test specimen and the frame; force H6 in particular may significantly influence the total skewing of the wall element depicted in Fig.10. The discrepancies between the measured and calculated forces can be explained by the unequal setting of the adjustable bolts. The calculation also demonstrated the strong influence of the stiffness of the frame on the amount of total skewing. It is clear from Fig.9 that the rotation of the element caused by deformation of the test apparatus contributes to the total skewing by more than 50%.

The good correlation with the measured values is shown by the skewing of the monitored sections in Fig.12.

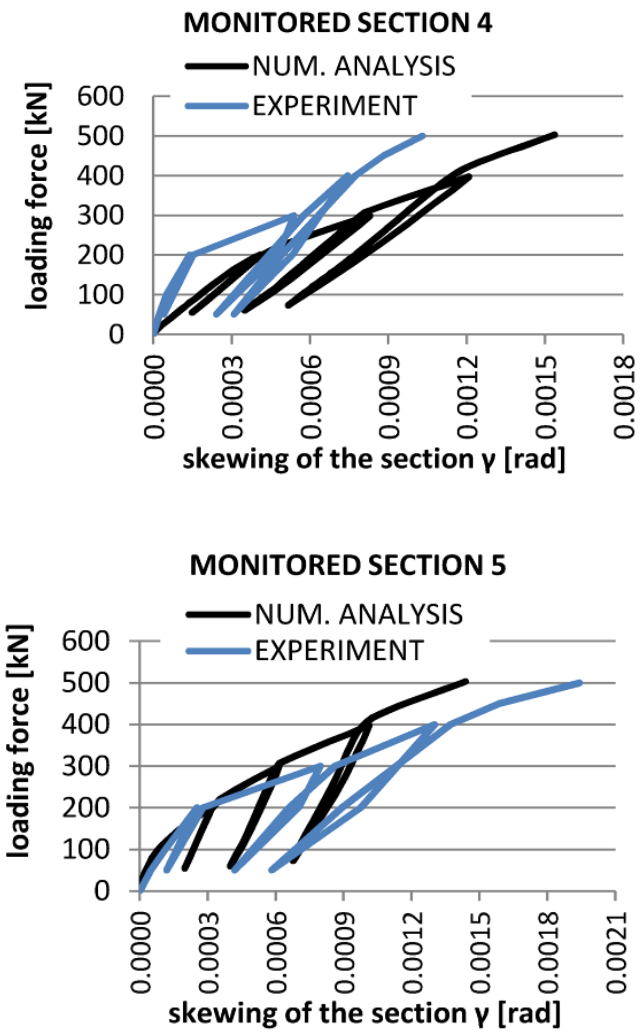

Fig. 13 – Dependence of skewing on loading force for monitored section No.4 (top) and No.5 (bottom)

During the performance of the tests cyclic loading was applied with a set time step for each loading and unloading. With regard to the fact that the numerical computation does not include any rheological phenomena, the real course of the cyclic loading was simplified, see Fig.6. Loading is produced via the application of force on the load distribution arm and the upper part of the frame, just as the hydraulic loading device acts on a real structure.

ACKNOWLEDGMENT

This result was achieved with the financial support of the project GACR 14-25320S "Aspects of the use of complex nonlinear material models".

REFERENCES

[1] Ahmad, S.I., Tanabe, T.-A., "Three-dimensional FE analysis of reinforced concrete structures using the lattice equivalent continuum method," *Structural Concrete*, 14 (1), pp. 51-59, 2013.
[2] ANSYS Theory Release 15.1, ANSYS Inc., 2014.
[3] Bažant, Z.P., Oh, B.H., "Crack band theory for fracture of concrete," *Materials and Structures*, RILEM, 93 (16), pp. 155-177, 1993.
[4] Belletti, B., Damoni, C., Hendriks, M.A.N., De Boer, A., "Analytical and numerical evaluation of the design shear resistance of reinforced concrete slabs," *Structural Concrete*, 15 (3), pp. 317-330, 2014.
[5] Bennani, M.A., El Akkad, A., Elkhalfi, A., "Mixed finite element method for linear elasticity in a cracked domain," *WSEAS Transactions on Applied and Theoretical Mechanics*, 9, pp. 167-178, 2014.
[6] Chen, W.F., *Constitutive Equations for Engineering Materials, Vol. 2 Plasticity and Modeling*. Elsevier Amsderdam - London - New York – Tokyo, 1994.
[7] Holomek, J., Bajer, M., "Experimental and Numerical Investigation of Composite Action of Steel Concrete Slab," *Procedia Engineering*. 2012(40), pp. 143 – 147, ISSN 1877-7058.
[8] Hradil, P., Kala, J., "Analysis of the shear failure of a reinforced concrete wall," *Applied Mechanics and Materials*, 621, pp. 124-129, 2014.
[9] Huang, J.-Y., "Dynamic analysis of cracks running at a constant velocity in a strip," *WSEAS Transactions on Applied and Theoretical Mechanics*, 6 (2), pp. 49-58, 2011.
[10] Jianga, H., Kurama, Y. C., "An analytical investigation on the seismic retrofit of older medium-rise reinforced concrete shear walls under lateral loads," *Engineering Structures*, Volume 46, January 2013, 459–470, doi. 10.1016/j.engstruct.2012.08.007, 2013.
[11] Kala, Z., Kala, J., "Resistance of thin-walled plate girders under combined bending and shear," *WSEAS Transactions on Applied and Theoretical Mechanics*, 5 (4), pp. 242-251, 2010.
[12] Karmazínová, M., Melcher, J., "Initial imperfections of steel and steel-concrete composite columns subjected to buckling compression," *WSEAS Transactions on Applied and Theoretical Mechanics*, 9, pp. 27-34, 2014.
[13] Magnusson, J., Hallgren, M., Ansell, A., "Shear in concrete structures subjected to dynamic loads," *Structural Concrete*, 15 (1), pp. 55-65, 2014.
[14] MultiPlas, *User's Manual Rev. 10 Release 4.1.0 for ANSYS 13*, Dynardo, Weimar, Germany, www.dynardo.de, 2010.
[15] Ottosen N.S., "A Failure Criterion for Concrete," *Journal of the Engineering Mechanics Division*, Vol. 103, No. 4, pp. 527-535, July/August, 1977.
[16] Park, R., Paulay, T., *Reinforced Concrete Structures*, Wiley, New York, 1975.
[17] Paulay, T., Priestley, M. J. N., *Seismic Design of Reinforced Concrete and Masonry Buildings*, Wiley, New York, 1992.
[18] Rangan, B. V., "Shear Design of Reinforced Concrete Beams, Slabs and Walls," *Cement and Concrete Composites*, 20, 455-464, Elsevier Science, 1998.
[19] Topcu, I.B., Bilir, T., Boga, A.R., "Estimation of the modulus of elasticity of slag concrete by using composite material models", *Construction and Building Materials* 24, 741–748, 2010.